EXAMINING THE INFLUENCE OF SALTWATER INTRUSION ON MANGROVE BIOMASS IN THE CAN GIO BIOSPHERE RESERVE (1993–2023): INSIGHTS FROM SUN-GLINT CORRECTED SATELLITE IMAGERY

CHU, H. X.[1] – LE, T. Q.[1] – NGUYEN, N. M.[1] – TONG, A. H. T.[1] – BUI, H. Q.[1] – HOANG, H.[1] – NGUYEN, H. P.[1] – NGUYEN, H. D.[1] – DO, A. N. T.[2,3*]

[1]*Space Technology Institute, Vietnam Academy of Science and Technology, 18 Hoang Quoc Viet, Cau Giay, Ha Noi, Vietnam*

[2]*Laboratory of Ecology and Environmental Management, Science and Technology Advanced Institute, Van Lang University, Ho Chi Minh City, Vietnam*

[3]*Faculty of Applied Technology, School of Technology, Van Lang University, Ho Chi Minh City, Vietnam*

[*]*Corresponding author*
e-mail: dothingocanh@vlu.edu.vn; ORCID ID: orcid.org/0000-0002-2926-526X

(Received 7th Sep 2024; accepted 9th Dec 2024)

Abstract. Salinity serves as a pivotal determinant in the growth and progression of mangrove forests. This study aims to investigate the impact of saline intrusion on the aboveground biomass (AGB) of the Can Gio mangrove forest from 1993 to 2023. Notably, the AGB has experienced a decline primarily due to escalating saline water intrusion. However, the coastal area is always subject to waves and wind, which create an uneven sea surface and result in sun glint. Sun glint alters the reflectance spectrum values and often occurs in high-resolution satellite images, leading to significant distortions. To enhance the accuracy of satellite imagery results, this research innovatively utilized satellite image data that has been corrected for sun glint, addressing the adverse effects of solar radiation. Based on the urgency of the project in the current context, this study employed the SVM-XGBoost-1 and SVM-XGBoost-2 (Support Vector Machine- Extreme Gradient Boosting) hybrid models to estimate the AGB and salinity of the Can Gio mangrove forest, thus establishing a correlation between these two variables. The hybrid models exhibited superior performance compared to non-optimized models, with Coefficient of Determination (R^2) value exceeding 0.83 and a reduction in Root Mean Square Error (RMSE) to 4.982 and 3.026, respectively. The computed results showcase an inverse proportional relationship, wherein an increase in salinity results in a decrease in the AGB of the Can Gio mangrove forest. The fringe region, where saltwater and freshwater merge and interact with human disturbances, along with areas possessing biomass reserves of 150 or more, are notably affected. This underscores the substantial impact of saline intrusion on the reduction of AGB over the past three decades. The findings from this study provide valuable insights for managers, equipping them with the necessary information to implement effective conservation measures for the Can Gio mangrove biosphere reserve.
Keywords: *above ground biomass, salinity, remote sensing, machine learning, Rhizophora apiculata*

Introduction

Mangrove forests denote distinct natural ecosystems that play a pivotal role not only in the economic and ecological spheres but also in the environmental aspects of coastal wetland areas in tropical and subtropical regions (Do et al., 2022a,b). The survival, growth, development, and distribution of these forests are intricately linked to the inherent conditions, topography, and geomorphology of their habitats (Feller et al., 2010; Biswas and Biswas, 2021). Modifications in the environmental conditions of wetland areas will

http://www.aloki.hu ● ISSN 1589 1623 (Print) ● ISSN1785 0037 (Online)
DOI: http://dx.doi.org/10.15666/aeer/2301_16351658

inevitably lead to fluctuations within mangrove forest ecosystems to some degree (Ward et al., 2016; Jennerjahn et al., 2017). Therefore, it becomes necessary to examine and ascertain the impact of environmental factors, such as salinity, on the development of mangrove forests to establish a scientific foundation for proposing appropriate species selection and sustainable reforestation solutions for protective forests along coastlines.

Salinity is an essential factor that significantly affects the growth and survival rate of plant species and the distribution of mangrove forests. This factor is closely associated with the osmotic pressure, as mentioned by Kodikara et al. (2017); and Parida et al. (2004). As salinity levels rise, the corresponding increase in osmotic pressure poses challenges for plant roots in absorbing water (Dittmann et al., 2022). Each species of mangrove tree exhibits a unique tolerance range towards salinity. When the salinity level is suitable for a specific species, it thrives and flourishes. However, excessive salinity can impede the growth of trees and even lead to their demise (Suárez and Medina, 2005; Shiau et al., 2017). Numerous studies have been conducted on the intrusions of saline water and the aboveground biomass (AGB) of mangrove forests. However, these studies often treat these two issues separately and fail to establish clear spatial and temporal relationships. Instead, they predominantly rely on statistical measurements (Liang et al., 2008; Noor et al., 2015; Do et al., 2022b).

Traditional methods for studying AGB primarily involve direct measurements of tree height, tree area, and diameter at breast height. Biometric equations are then utilized to calculate the total AGB (Pham and Yoshino, 2017; Laurin et al., 2018; Do et al., 2022b). Nevertheless, these traditional methods encounter challenges such as time and labor intensiveness, limitations in small-scale areas, and difficulties in estimating AGB when trees are closely spaced (Clough and Scott, 1989). On the other hand, remote sensing methods have demonstrated greater advantages compared to traditional methods in surveying and studying the distribution and structure of mangrove forests (Do et al., 2022b). These remote sensing applications also facilitate the determination of tree height and the estimation of AGB over a wide range. Nonetheless, there is a limited number of studies that have employed sun glint-corrected satellite images to enhance the precision of data extraction from satellite images (Kay et al., 2009). Notably, NAM (2019); and Sharifi and Hosseingholizadeh (2020) have emphasized the efficacy of remote sensing in these aspects.

Saline water intrusion is an intricate and unpredictable phenomenon that has a profound impact on vast regions (Fang et al., 2019). Nevertheless, the monitoring, analysis, and early warning systems employed to address saline water intrusion continue to be hindered by the limitations posed by sparse and outdated monitoring networks. The investigation of saline intrusion predominantly relies on conventional techniques such as field measurements and sampling, which are characterized by their high cost, time-consuming nature, labor-intensive requirements, and delayed provision of information for early warning systems (Allbed et al., 2014; Alexakis et al., 2018). Remote sensing technology, equipped with its multispectral and multitemporal imagery, possesses the ability to monitor alterations across a wide expanse without being constrained by the number of monitoring stations (Huete et al., 1994). Recently, machine learning methods have been leveraged to extract information from remote sensing data and achieve remarkable precision (Vermeulen and van Niekerk, 2016; Alexakis et al., 2018).

In contemporary research, machine learning models have emerged as potent instruments for analyzing and forecasting the intricate relationships among environmental variables (Do and Tran, 2023a,b,c; Pham et al., 2023). A multitude of robust algorithms

http://www.aloki.hu ● ISSN 1589 1623 (Print) ● ISSN1785 0037 (Online)
DOI: http://dx.doi.org/10.15666/aeer/2301_16351658

have been deployed in tackling nonlinear regression problems, with the Extreme Gradient Boosting (XGBoost) algorithm emerging as particularly noteworthy (Pham et al., 2023). However, the utilization of an extensive array of inputs for the model can potentially result in overfitting. Notably, Support Vector Machines (SVM) are distinguished for their proficiency in managing high-dimensional data and effectively categorizing nonlinear relationships, rendering them exceptionally appropriate for ecological investigations characterized by complex variable interactions (Do et al., 2022b; Do and Tran, 2023a). Hence, in this present study, SVM algorithm has been employed to enhance the performance of the prediction model (Do et al., 2022b; Do and Tran, 2023a). In comparison to conventional machine learning approaches, hybrid SVM-XGBoost models exhibit superior performance in regression tasks, possessing the ability to address missing data and implementing modifications to mitigate overfitting. This enhances the precision of assessments concerning salinity and above-ground biomass (AGB) of mangroves under fluctuating environmental conditions (Do et al., 2022b; Pham et al., 2023). Consequently, the SVM-XGBoost-1 and SVM-XGBoost-2 models were utilized to estimate the Above-Ground Biomass (AGB) and salinity levels of mangrove forests, respectively.

In recent times, saline intrusion has emerged as a formidable challenge for mangrove forests in diverse regions across the globe (Mitra et al., 2010). Such changes not only influence the progression of mangrove forests but also have repercussions for communities reliant on resources from these ecosystems. Despite extensive research on saline intrusion and AGB of mangroves, the majority of studies have tended to treat these topics independently, lacking a definitive spatial and temporal correlation (Do et al., 2022b). Consequently, investigating and evaluating the repercussions of saline intrusion on mangrove ecosystems represents not only a critical scientific imperative but also a vital component for formulating conservation policies and sustainable management practices. The principal aim of this study is to assess the effects of saline intrusion on mangrove biomass within the Can Gio Biosphere Reserve, Vietnam, spanning the years from 1993 to 2023. The focus will be on elucidating the correlation between the extent of saline intrusion and the biomass of mangrove forests, thereby offering insights into how environmental factors shape the growth and distribution of mangroves. In this manner, the study will furnish a scientific foundation for devising more effective conservation interventions, ensuring the sustainability and proliferation of mangrove ecosystems amidst escalating saline intrusion. The findings from this research will be relevant to other mangrove regions with comparable environmental conditions, thus providing crucial data for conservation initiatives in the face of climate change and increasing salinity levels.

Materials and methods

Study area and data sources

Study site

The Can Gio Mangrove Biosphere Reserve is formed in the downstream of the Dong Nai - Saigon river system, located at the southeastern gateway of Ho Chi Minh City. Coordinates: 10°22' - 10°40' north latitude and 106°46' - 107°01' east longitude (*Figure 1*). It is approximately 60 km away from the city center of Ho Chi Minh City. The Can Gio Biosphere Reserve borders Nhon Trach district, Long Thanh district (Dong Nai province), Chau Thanh district, Ba Ria town, Vung Tau city (Ba Ria - Vung Tau province) to the east and northeast; Can Duoc district, Can Giuoc district (Long An

http://www.aloki.hu ● ISSN 1589 1623 (Print) ● ISSN1785 0037 (Online)
DOI: http://dx.doi.org/10.15666/aeer/2301_16351658

province), Go Cong Dong district (Tien Giang province) to the west; and Nha Be district (Ho Chi Minh City) to the northwest. It is also adjacent to the East Sea to the south. The length of the Can Gio Biosphere Reserve from north to south is 35 km, and from east to west is 30 km, with over 20 km of coastline running in the southwest-northeast direction. The Can Gio Biosphere Reserve is entirely within the administrative boundaries of Can Gio district, with a total area of 75,740 ha. Due to the significant conservation value of the Can Gio mangrove forest, it was recognized by UNESCO as a "Biosphere Reserve" in 2000.

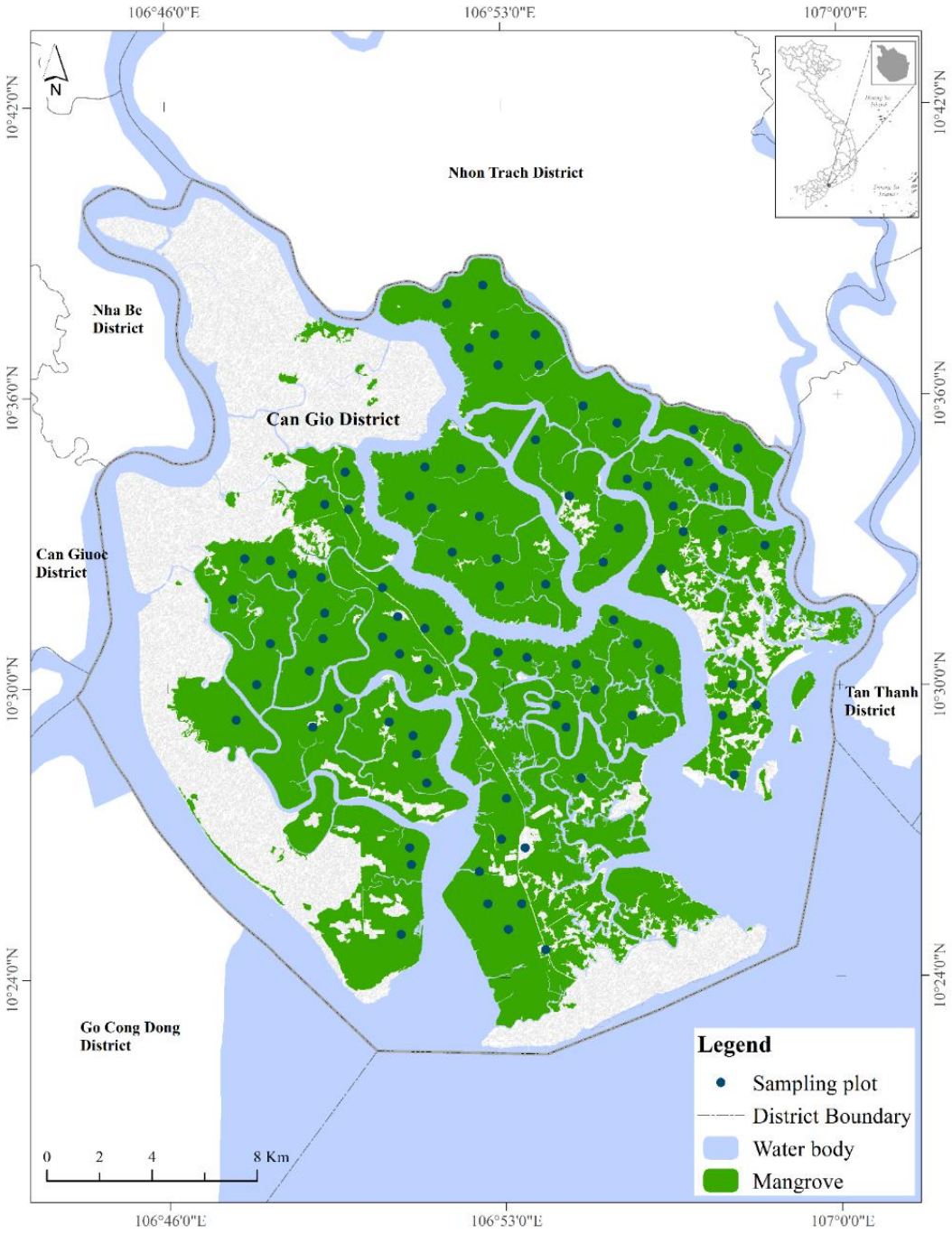

Figure 1. *An illustration of the research area at Vietnam's Can Gio district's Can Gio mangrove biosphere reserve*

http://www.aloki.hu ● ISSN 1589 1623 (Print) ● ISSN1785 0037 (Online)
DOI: http://dx.doi.org/10.15666/aeer/2301_16351658

This area has a tropical monsoon climate, with two distinct seasons of rain and sunshine. The rainy season typically occurs from May to October, while the dry season extends from November to April of the following year. The Can Gio mangrove forest is characterized by distinctive environmental conditions, functioning as a transitional ecosystem between aquatic and terrestrial habitats, as well as between freshwater and saltwater environments. As it is located in the river mouth region, it is directly influenced by the semi-diurnal tidal regime from the East Sea. The rivers and canals in Can Gio district play the role of "tidal conduits" that allow saline water to infiltrate throughout the district, causing the surface water here to be saline throughout the year. This forest receives substantial sediment influx from the Dong Nai River, coupled with influences from the nearby sea and tidal variations, culminating in a rich plant diversity exceeding 150 species. This biodiversity offers sustenance and habitat for a multitude of aquatic species, fish, and other vertebrates (Do et al., 2022b). However, the encroachment of saltwater from the sea into inland territories is a pivotal factor influencing the development of mangrove forests. Elevated salinity levels can adversely affect the biomass and growth of mangrove species.

Data collection

The current study established 90 standard plots, each with an area of 100 m^2 each (*Figure 1*). Nevertheless, a sample plot size of 100 m^2 may not adequately capture biomass variations in regions exhibiting extremely high or low tree density. Therefore, this study has amassed a substantial sample size and systematically and randomly distributed sample plots, integrated with satellite technology. Each point on the map represents the coordinates of the center of each standard plot, which were randomly selected to ensure representation of different mangrove forest types within the Can Gio Biosphere Reserve. In each standard plot, the following data were collected:

- Density: Counting all live trees within each standard plot (n);
- Diameter at Breast Height (DBH): Measuring the diameter of the tree trunk at a height of 1.3 meters above the ground using calipers;
- Height (h): Measuring the height of the tree using a measuring tape with an accuracy of 0.1m;
- Dry-to-fresh biomass ratio = W_{di}/W_{fi}

where W_{di} is the dry weight of the stem, branches, and leaves after drying at 105°C; and W_{fi} is the fresh weight of the stem, branches, and leaves of the tree before drying.

Estimating the aboveground biomass (AGB) of different mangrove forests in the Can Gio Mangrove Biosphere Reserve relies on the following general formula (Do et al., 2022b):

$$AGB = a \times DBH_{1.3}^{b} \quad \text{(Eq.1)}$$

where $DBH_{1.3}$ represents the diameter at breast height at a tree height of 1.3 m; and a, and b are coefficients that vary depending on the type of forest and the main components of the tree, such as trunk, canopy, or leaves.

Data were collected during the dry season in January over the span of four years. By focusing on a single month across different years, the study aims to reduce the variability introduced by seasonal changes, thereby providing a clearer understanding of long-term trends in biomass and salinity within the mangrove ecosystem. The EM-38 device is utilized to obtain the salinity measurement data, and the salinity is calculated based on

http://www.aloki.hu ● ISSN 1589 1623 (Print) ● ISSN1785 0037 (Online)
DOI: http://dx.doi.org/10.15666/aeer/2301_16351658

the electrical conductivity (EC) measured in dS/m. In this particular investigation, 70% of the samples are employed for model computation, while the remaining 30% are utilized for validating the model predictions. These samples are considered as dependent variables, whereas the independent variables are derived from Landsat satellite imagery.

Pre-processing and sun-glint-correction of optical satellite images

Satellite sensors may encounter various influences such as sensor characteristics, solar energy, atmosphere, and the terrain of the area, which can affect the acquired satellite images (Do, 2024a; Do et al., 2022, 2023; Pham et al., 2023). Consequently, the objective of satellite image preprocessing is to minimize these influences to the greatest extent possible. In this study, all multitemporal satellite data are corrected for radiation/atmospheric influences on surface reflectance using the ATCOR method (Do et al., 2022b; Pham et al., 2024) integrated into CATALYST Professional software, which facilitates the restoration of the atmospheric-affected components. Subsequently, all satellite data are georeferenced to the VN2000 coordinate system, ensuring a positional accuracy of less than ±0.5 pixel.

Lyzenga sun glint correction method

Instead of using regression, Lyzenga employs the covariance between the visible and NIR channels to establish the relationship between them, sampling regions similar to the Hedley method (Lyzenga et al., 2006). The covariance of two random variables x, y, denoted as Cov(x,y), represents the mathematical expectation of the product of the deviations of those random variables from their mathematical expectation. It is calculated using the following formula:

$$\mathrm{Cov}(x,y) = E(x - Ey)\,(y - Ey) = Exy - Ex\,Ey \qquad \text{(Eq.2)}$$

The covariance between two variables can be negative, positive, or zero. A positive covariance indicates movement in the same direction, while a negative covariance indicates movement in opposite directions. A covariance of zero signifies no linear relationship between the variables.

When applied to two channels - visible channel (i) and NIR channel (j), with N as the number of pixels in the sample area - the covariance between the two channels is determined as follows:

$$\mathrm{Cov}(i,j) = \frac{1}{N}\sum_{n=1}^{N} L_{in}L_{jn} - \frac{1}{N}\sum_{n=1}^{N} L_{in}\,\frac{1}{N}\sum_{n=1}^{N} L_{jn} \qquad \text{(Eq.3)}$$

where, the coefficient used to adjust sun glint r_{ij} is calculated as:

$$r_{ij} = \mathrm{Cov}(i,j)/\mathrm{Cov}(j,j) \qquad \text{(Eq.4)}$$

where, $\mathrm{Cov}(j,j)$ represents the covariance of the near-infrared channel.

dR_{VIS} is calculated as follows:

$$dR_{VIS} = r_{ij}(R_{NIR} - \mathrm{Mean}_{NIR}) \qquad \text{(Eq.5)}$$

http://www.aloki.hu ● ISSN 1589 1623 (Print) ● ISSN1785 0037 (Online)
DOI: http://dx.doi.org/10.15666/aeer/2301_16351658

where VIS refers to the visible channel, R_{NIR} is the pixel value on the NIR channel, and $Mean_{NIR}$ is the average value of the deepwater sample pixels on the NIR channel.

The sun glint correction is then determined as

$$R'_{VIS} = R_{VIS} - dR_{VIS} \quad \text{(Eq.6)}$$

By combining equations (5) and (6):

$$R'_{VIS} = R_{VIS} - r_{ij}(R_{NIR} - Mean_{NIR}) \quad \text{(Eq.7)}$$

Satellite images post-preprocessing and sun glint correction are depicted in *Figure 2.*

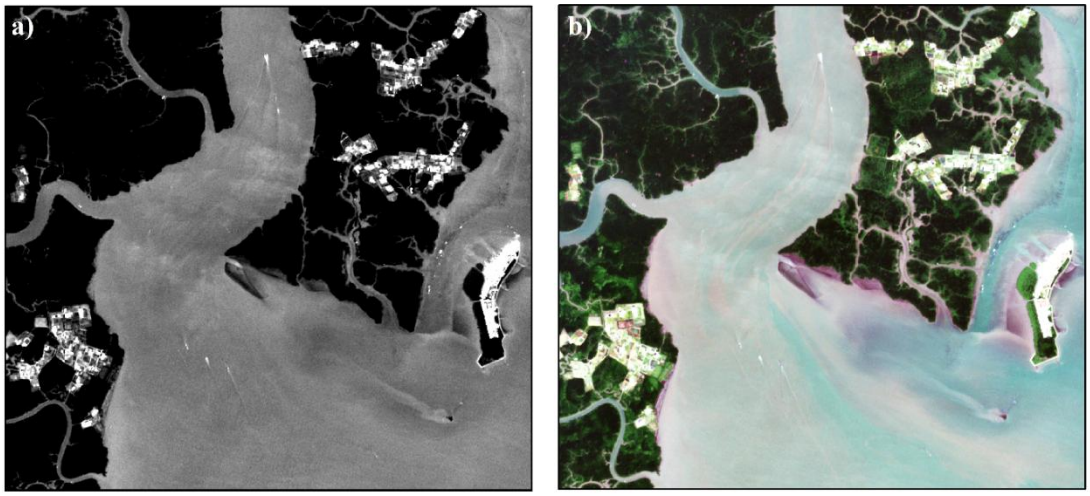

Figure 2. *Satellite images before (a) and after (b) preprocessing and sun glint correction.*

Four LANDSAT images corresponding to four study years are collected in this investigation, namely Landsat 5 (1993), Landsat 7 (2003), Landsat 7 (2013), and Landsat 9 (2023), all captured during the dry season in January. The Landsat image series allows for tracking the changes in AGB, and salinity over time, at different time points, thereby providing accurate insights into the impact of saltwater intrusion on mangrove AGB.

XGBoost model in predicting salinity and mangrove AGB

Extreme gradient boosting (XGBoost), introduced by Chen et al. (2015), is a novel classification method. The underlying concept of XGBoost is to create a series of weak learner models that complement each other (Do and Tran, 2023b). In other words, subsequent models in XGBoost aim to learn from and rectify the mistakes made by the preceding models, specifically focusing on the data that was incorrectly predicted by the previous model. This sequential process results in a sequence of models, with each subsequent model improving upon its predecessor by adjusting the weights based on the data. Compared to other traditional algorithms, XGBoost often exhibits better performance, particularly when dealing with large and complex datasets. Notably, the weights of correctly predicted data remain unchanged, while the weights of incorrectly predicted data are increased. XGBoost is an optimized version of the Gradient Boosting machine. In gradient boosting, decision trees are constructed sequentially, and each new

http://www.aloki.hu ● ISSN 1589 1623 (Print) ● ISSN1785 0037 (Online)
DOI: http://dx.doi.org/10.15666/aeer/2301_16351658

model employs the gradient descent algorithm (Chen et al., 2019). Therefore, it is capable of functioning effectively even in scenarios involving missing data.

The XGBoost model can be computed using the following general formula (Chen and Guestrin, 2016):

$$y_i' = \gamma(x_i) = \sum_{k=1}^{k} f_k(x_j), \quad f_k \epsilon F \tag{Eq.8}$$

where F is the function space, x_i an n-dimensional input vector, y_i' is the prediction function. To construct the set of functions used in the model, the following objective function is employed:

$$L(\gamma) = \sum_i l(y_i', y_i) + \sum_k \omega(f_k) \tag{Eq.9}$$

with $\omega(f_k) = \rho T + \frac{1}{2}\tau\|w\|^2$.

Optical imagery offers valuable insights into the state of mangrove forests by enhancing the contribution of vegetation characteristics or chemical components of leaves through the conversion of spectral bands (Do et al., 2022b). The present study employs 22 distinct vegetation indices and the XGBoost-1 model to estimate aboveground biomass (AGB) (*Table 1*).

Salinity is found to be correlated with visible to near-infrared channels based on spectral reflectance characteristics. Consequently, salt types such as sodium sulfate, halite, gypsum, calcium carbonate, and sodium bicarbonate exhibit strong reflectance (over 80%) within the wavelength range of 0.4 to 1.4μm (Westin and Nissling, 1991; Davis et al., 2019). Therefore, 13 variables from the visible to near-infrared channels have been chosen as inputs for the XGBoost-2 model to estimate salinity in the study area (*Table 2*).

Improving model performance with SVM algorithm

Although the XGBoost algorithm is a powerful tool for classification and regression tasks, the presence of numerous variables can result in overfitting, leading to model errors. To enhance the model's performance, the Support Vector Machine (SVM) algorithm is employed in the current study. SVM constitutes a set of supervised methods that can identify optimal models in a multi-dimensional space (Do et al., 2022b; Do and Tran, 2023a).

Assuming the training data is represented by $\{x_i, y_i\}$, i = 1…k, where $x \in R^n$ is an n-dimensional vector in the feature space and $y \in \{-1, 1\}$ is the class label. This training data can be separated if there exists a vector $w = (w_1 \ldots w_2)$ and a scalar b that satisfy the following inequality:

$$y_i(wx_i + b) - 1 + \aleph_i \geq 0 \quad \forall y = \{1, -1\} \tag{Eq.10}$$

where $\aleph_i$ indicates the distance of the data point to the optimal model. The objective function can be written as follows:

$$\|w\|^2 + C\sum_i = 1^k \aleph_i \tag{Eq.11}$$

http://www.aloki.hu ● ISSN 1589 1623 (Print) ● ISSN1785 0037 (Online)
DOI: http://dx.doi.org/10.15666/aeer/2301_16351658

Table 1. *Predictor variables from Landsat satellite*

No.	Index	Name/Explanation	Formula	Reference
1	B1	Blue	$BLUE$	(Chandra et al., 2011; Do et al., 2022b; Pham et al., 2023)
2	B2	Green	$GREEN$	
3	B3	Red	RED	
4	B4	NIR	NIR	
5	RECI	Red-edge Chlorophyll index	$\frac{NIR}{RED-Edge}-1$	
6	GCI	Green Chlorophyll index	$\frac{NIR}{GREEN}-1$	
7	GSAVI	Green soil adjusted vegetation index	$1.5\frac{NIR-GREEN}{NIR+GREEN+0.5}$	
8	GRVI	Green red vegetation index	$\frac{GREEN-RED}{GREEN+RED}$	
9	EVI	Enhanced vegetation index	$\frac{2.5\times(NIR-RED)}{1+NIR+6RED-7.5BLUE}$	
10	NDVI	Normalized difference vegetation index	$\frac{NIR-RED}{NIR+RED}$	
11	OSAVI	Optimized soil adjusted vegetation index	$\frac{NIR-RED}{NIR+RED+0.16}$	
12	PBI	Plant biochemical index	$\frac{NIR}{GREEN}$	
13	PVI	Perpendicular vegetation index	$\frac{1}{\sqrt{a^2+1}}(NIR-a\times RED-b)$ where a, and b are the slope and gradient of the soil line, respectively.	
14	SAVI	Soil adjusted vegetation index	$1.5\frac{(NIR-RED)}{NIR+RED+0.5}$	
15	TVI	Transformed vegetation index	$\sqrt{NDVI+0.5}$	
16	WDVI	Weighted difference vegetation index	$NIR-a\times RED$	
17	ARVI	Atmospherically resistant vegetation index	$\frac{NIR-RED-y(RED-BLUE)}{NIR+RED-y(RED-BLUE)}$	
18	GARI	Green atmospherically resistant vegetation index	$\frac{NIR-(GREEN-(BLUE-RED))}{NIR-(GREEN+(BLUE-RED))}$	

http://www.aloki.hu ● ISSN 1589 1623 (Print) ● ISSN1785 0037 (Online)
DOI: http://dx.doi.org/10.15666/aeer/2301_16351658

No.	Index	Name/Explanation	Formula	Reference
19	CI	Coloration index	$\frac{\mathrm{RED}-\mathrm{BLUE}}{\mathrm{RED}}$	
20	CVI	Chlorophyll vegetation index	$\mathrm{NIR}\frac{\mathrm{RED}}{\mathrm{GREEN}^2}$	
21	GI	Greenness index	$\frac{\mathrm{GREEN}}{\mathrm{RED}}$	
22	MSAVI	Modified soil adjusted vegetation index	$\frac{2\mathrm{NIR}+1-\sqrt{(2\mathrm{NIR}+1)^2-8(\mathrm{NIR}-\mathrm{RED})}}{2}$	

http://www.aloki.hu ● ISSN 1589 1623 (Print) ● ISSN1785 0037 (Online)
DOI: http://dx.doi.org/10.15666/aeer/2301_16351658

Table 2. *Selected indicators to calculate salinity for the study area*

Index	Formula	Reference
Soil brightness index	$\mathrm{SBI} = \sqrt{\mathrm{GREEN}^2 + \mathrm{NIR}^2}$	(Westin and Nissling, 1991; Allbed et al., 2014; Alexakis et al., 2018; Tran et al., 2018)
Normalized difference salinity index	$\mathrm{NDSI} = (\mathrm{RED} - \mathrm{NIR})/(\mathrm{RED} + \mathrm{NIR})$	
Vegetation soil salinity index	$\mathrm{VSSI} = 2 \times \mathrm{GREEN} - (5 \times (\mathrm{RED} + \mathrm{NIR}))$	
Normalized soil index	$\mathrm{NSI} = \frac{\mathrm{SWIR1} - \mathrm{SWIR2}}{\mathrm{SWIR1} - \mathrm{NIR}}$	
Soil Adjusted Vegetation Index	$\mathrm{SAVI} = 1.5 \times \frac{\mathrm{NIR} - \mathrm{RED}}{0.5 + \mathrm{NIR} + \mathrm{RED}}$	
Salinity index 1	$\mathrm{SI1} = \sqrt{\mathrm{GREEN} \times \mathrm{RED}}$	
Salinity index 2	$\mathrm{SI2} = \sqrt{\mathrm{GREEN}^2 + \mathrm{RED}^2 + \mathrm{NIR}^2}$	
Salinity index 3	$\mathrm{SI3} = \sqrt{\mathrm{GREEN}^2 \times \mathrm{RED}^2}$	
Salinity index 4	$\mathrm{SI4} = \mathrm{RED}/\mathrm{NIR}$	
Salinity index 5	$\mathrm{SI5} = \mathrm{SWIR1}/\mathrm{SWIR2}$	
Intensity 1	$\mathrm{INT1} = (\mathrm{GREEN} + \mathrm{RED})/2$	
Intensity 2	$\mathrm{INT2} = (\mathrm{GREEN} + \mathrm{RED} + \mathrm{NIR})/2$	
Enhanced vegetation index	$\mathrm{EVI} = 2.5 \times \left(\frac{(\mathrm{NIR} - \mathrm{RED})}{(\mathrm{NIR} + 6 \times \mathrm{RED} - 7.5 \times \mathrm{BLUE} + 1)}\right)$	

The basic approach to SVM classification can be extended to allow for nonlinear decision boundaries by mapping the input data into a higher-dimensional feature space H. To achieve this, a kernel function is proposed: $\mathrm{K}(\mathrm{x_i}, \mathrm{x_j}) = \left(\varphi(\mathrm{x_i}), \varphi(\mathrm{x_j})\right)$, where an input data sample x can be represented as the vector $\varphi(\mathrm{x})$ in the feature space H. This kernel allows for the computation of the inner product of $\left(\varphi(\mathrm{x_i}), \varphi(\mathrm{x_j})\right)$ without explicitly knowing the exact representation of the data samples $\mathrm{x_i}$, and $\mathrm{x_j}$ in the higher-dimensional space.

In the current study, SVM is used to optimize the XGBoost-1 and XGBoost-2 models with the dependent variables for salinity estimation and mangrove aboveground biomass estimation in the Can Gio Mangrove Biosphere Reserve.

Evaluation of prediction model accuracy

The performance of the models is evaluated and compared using the Root Mean Square Error (RMSE) and Coefficient of Determination (R^2) indices (Do and Tran, 2023a,b,c; Pham et al., 2023, 2024; Do et al., 2024a; Van Pham et al., 2024). Both criteria assess the errors in the regression model based on the differences between the measured data and the estimated data.

$$\mathrm{RMSE} = \sqrt{\sum_{i=1}^{n} \frac{(\mathrm{ye_i} - \mathrm{ym_i})^2}{n}} \quad \text{(Eq.12)}$$

$$\mathrm{R^2} = \frac{\sum_{i=1}^{n} (\mathrm{ye_i} - \overline{\mathrm{ye}})(\mathrm{ym_i} - \overline{\mathrm{ym}})}{\sqrt{\sum_{i=1}^{n} (\mathrm{ye_i} - \overline{\mathrm{ye}})^2 (\mathrm{ym_i} - \overline{\mathrm{ym}})^2}} \quad \text{(Eq.13)}$$

http://www.aloki.hu ● ISSN 1589 1623 (Print) ● ISSN1785 0037 (Online)
DOI: http://dx.doi.org/10.15666/aeer/2301_16351658

where ye_i represents the variable predicted by the SVM-XGBoost model, ym_i is the measured field data, n is the total number of samples, $\overline{ye}$, and $\overline{ym}$ are the respective mean values of the predicted and measured data.

Results

SVM-XGBoost-1 in estimating mangrove AGB in Can Gio

In this current study, 22 variables were incorporated into the XGBoost-1 model. The findings indicate that the model yields relatively accurate predictions of mangrove aboveground biomass (AGB) with R^2>0.6, and RMSE=9.328 (*Table 3*).

Table 3. *Compare the performance between the XGBoost model and the model with improved performance using the SVM algorithm*

Model	R^2_{train}	R^2_{test}	R^2_{adj}	RMSE
XGBoost-1	0.633	0.622	0.617	9.328
SVM–XGBoost-1	0.848	0.836	0.830	4.982
XGBoost-2	0.659	0.648	0.621	5.223
SVM–XGBoost-2	0.863	0.858	0.840	3.026

This demonstrates the capability of the XGBoost-1 model to estimate AGB, although there is still a notable deviation from the actual values. To enhance the model's performance, the SVM algorithm is employed. Following 1000 iterations, the SVM-XGBoost-1 model achieves an RMSE value of 4.982, representing a reduction of 4.346 (almost twice) compared to the XGBoost-1 model (*Figure 3*). Furthermore, the R^2_{train}, R^2_{test}, and R^2_{adj} values are all above 0.8, specifically 0.848, 0.836, and 0.830, respectively (Table 3). These results indicate that the hybrid SVM-XGBoost-1 model outperforms the XGBoost-1 model, rendering it suitable for AGB estimation mapping in the Can Gio mangrove forest.

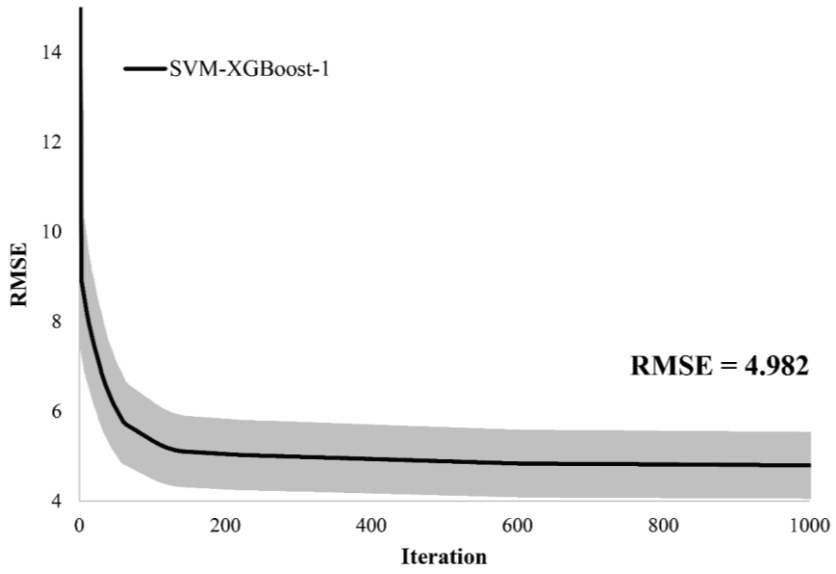

Figure 3. *The RMSE after 1000 tests was calculated from the SVM-XGBoost-1 model*

http://www.aloki.hu ● ISSN 1589 1623 (Print) ● ISSN1785 0037 (Online)
DOI: http://dx.doi.org/10.15666/aeer/2301_16351658

Figure 4 depicts the spatial distribution map of AGB in the study area utilizing the SVM-XGBoost-1 model. From 1993 to 2003, the area with AGB below 50 Mg/ha decreases from 6,381.273 ha to 3,835.272 ha (*Table 4*). This signifies habitat loss and a significant decline in the study area. Concurrently, the area with AGB ranging from 50 to 100 Mg/ha also decreases from 1,034.282 ha to 529.302 ha. However, from 2003 to 2023, this range experiences a substantial increase to 3,128.202 ha, indicating habitat recovery and biomass regeneration.

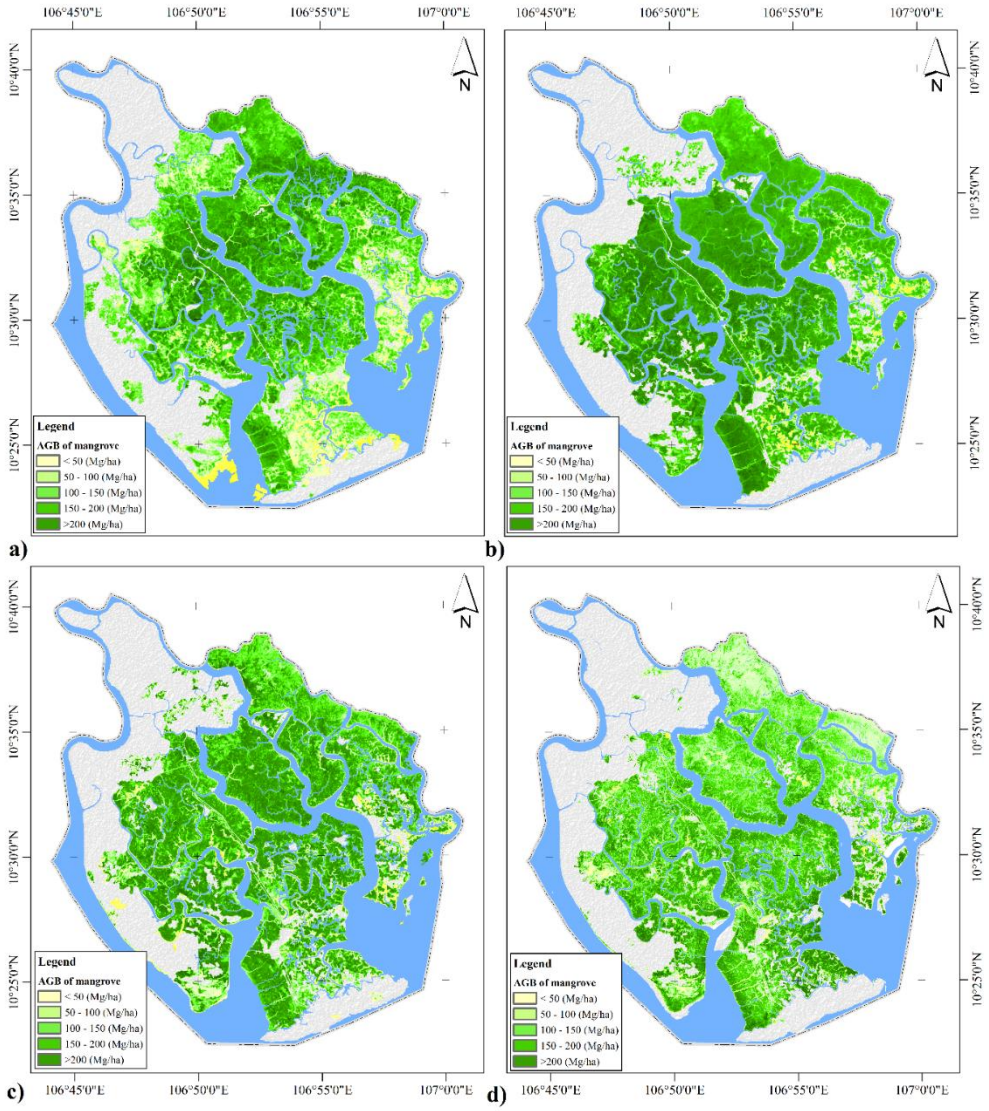

Figure 4. *Aboveground biomass of Can Gio mangrove forest. a) 1993; b) 2003; c) 2013; and d) 2023*

In 2003, the area with the highest biomass above 150 Mg/ha was documented, accounting for a total area of 26,273.555 ha (*Table 4*).

This can be attributed to the emphasis on reforestation efforts following the recognition of the Can Gio Mangrove Biosphere Reserve in 2000. By the years 2013 and 2023, AGB exhibited a declining pattern, particularly in the fringe areas where there is interaction with other land cover types, with the most notable decrease observed in the AGB>200

http://www.aloki.hu ● ISSN 1589 1623 (Print) ● ISSN1785 0037 (Online)
DOI: http://dx.doi.org/10.15666/aeer/2301_16351658

Mg/ha range. In 2023, this decline became even more pronounced, with the AGB 100–150 Mg/ha range representing the highest proportion (48.786% of the total area). This indicates a deterioration in habitat quality and the influence of climate change. Overall, the outcomes derived from the SVM-XGBoost-1 hybrid model reveal a substantial decrease in mangrove AGB in the Can Gio area over the past three decades, especially during the period from 2013 to 2023 (*Table 4*).

Table 4. *Area divided between each kind of mangrove AGB reserve between 1993 and 2023*

Biomass reserve (Mg/ha)	1993	2003	2013	2023
< 50	6,381.273	3,835.272	2,026.374	537.237
50–100	1,034.282	529.302	1,366.815	3,128.202
100–150	4,410.474	1,859.164	6,852.281	15,472.083
150–200	17,348.385	12,438.283	15,612.818	9,630.699
> 200	6,381.273	13,835.272	6,026.374	2,946.237
SUM	**35,555.690**	**32,497.291**	**31,884.662**	**31,714.456**

SVM-XGBoost-2 in salinity estimation

The SVM-XGBoost-2 model was employed to estimate salinity in the Can Gio mangrove forest and exhibited significantly superior performance compared to the XGBoost-2 model (*Table 3*). The RMSE value decreased from 5.223 to 3.026 after incorporating the SVM algorithm to enhance the performance of the XGBoost-2 model. The R^2>0.84 values surpassing 0.84 indicate a high level of accuracy in the model. Based on these calculations, the SVM-XGBoost-2 hybrid model was utilized to map the spatial and temporal distribution of salinity in the Can Gio mangrove forest from 1993 to 2023 (*Figure 5*).

During the period from 1993 to 2003, salinity in the mangrove forest experienced an upward trend. The maximum salinity value increased from 29.678 ppt to 30.456 ppt, while the minimum salinity value also rose from 10.345 ppt to 12.567 ppt (*Table 5*). This suggests a significant escalation in the intensity of salinity in the environment. The average salinity intensity also increased from 19.567 ppt to 21.789 ppt. Overall, during this period, an augmentation in salinity intensity in the mangrove forest can be observed, potentially attributed to factors such as seawater intrusion, surrounding environment, or climate change.

In the subsequent period from 2003 to 2013, salinity intensity continued to rise. The maximum and average values both increased to 31.789 and 22.012 ppt, respectively (*Table 5*). This increase indicates that the mangrove forest environment continues to be affected by higher salinity intensity. External factors such as environmental changes or human impacts may play a role in this increase. From 2013 to 2023, salinity intensity in the mangrove forest continued to slightly increase. The maximum value increased from 31.789 ppt to 34.567 ppt, while the minimum and average values rose to 12.901 ppt and 23.234 ppt, respectively (*Table 5*).

Overall, from 1993 to 2023, there has been an observed gradual increase in the intensity of salinity in the mangrove forest, as indicated in *Table 5*. In 1993, the maximum value for salinity intensity was recorded at 29.678 ppt, while the minimum value was 10.345 ppt. Over the course of 30 years, these values have increased to 34.567 ppt and 12.901 ppt, respectively. This gradual progression signifies the intrusion of saltwater in the mangrove forest over time.

http://www.aloki.hu ● ISSN 1589 1623 (Print) ● ISSN1785 0037 (Online)
DOI: http://dx.doi.org/10.15666/aeer/2301_16351658

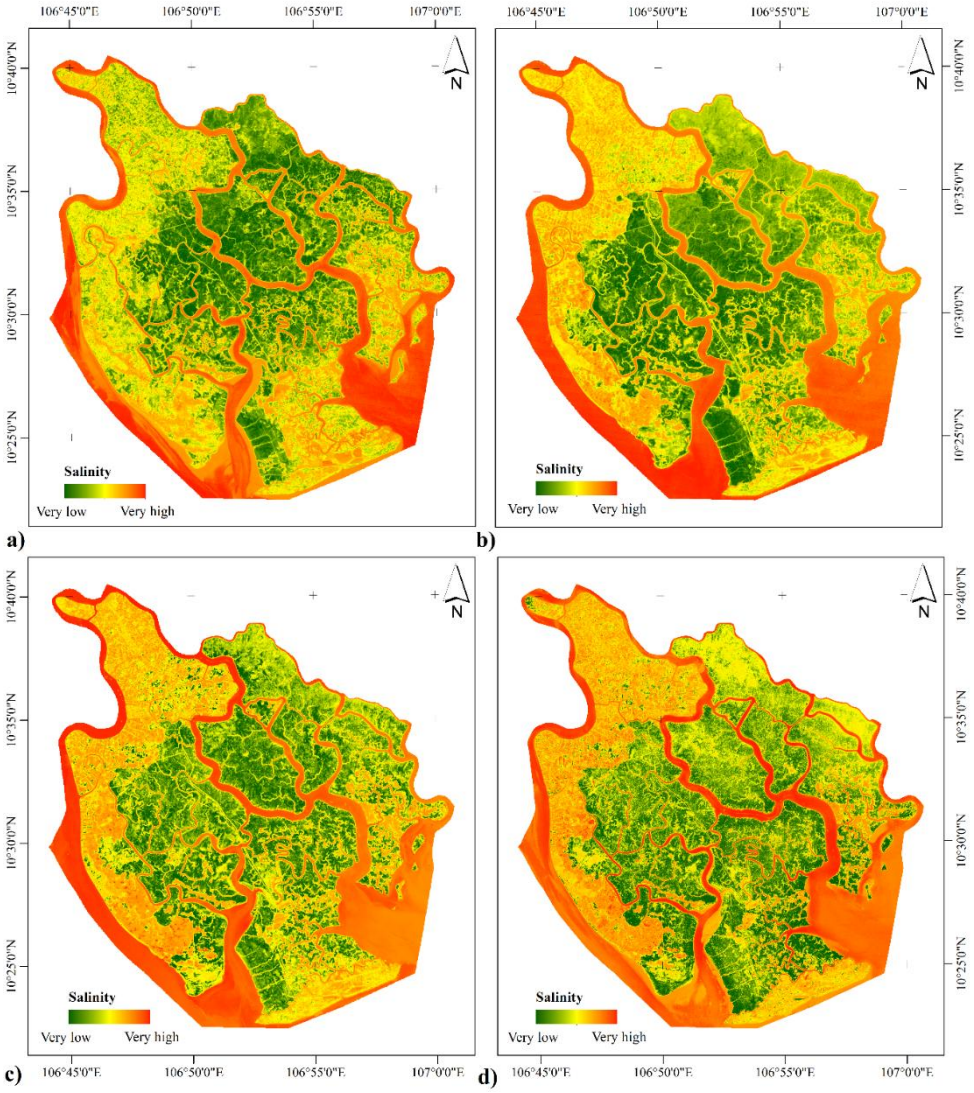

Figure 5. *The salinity of the mangrove forest is calculated from the hybrid model SVM-XGBoost-2. a) 1993; b) 2003; c) 2013; and d) 2023*

Table 5. *Salinity of the study area in the period 1993-2023 is calculated from the SVM-XGBoost-2 model*

Salinity (ppt)	Max	Min	Average
1993	29.678	10.345	19.567
2003	30.456	12.567	21.789
2013	31.789	11.234	22.012
2023	34.567	12.901	23.234

Assessing the impact of saltwater intrusion on mangrove AGB

Figure 6 illustrates the inverse relationship between salinity and AGB in the mangrove forest, with R=-0.729. Consequently, a strong inverse correlation between salinity and AGB has been determined. This implies that as salinity levels rise, the AGB in the mangrove forest decreases, and vice versa. The high salinity levels can have a detrimental

http://www.aloki.hu ● ISSN 1589 1623 (Print) ● ISSN1785 0037 (Online)
DOI: http://dx.doi.org/10.15666/aeer/2301_16351658

impact on the growth and development of vegetation and organisms in the mangrove forest, resulting in a decrease in biomass. In the section on estimating mangrove AGB, the decline in AGB over the 30-year period due to factors such as land, environment, and human activities has been extensively discussed. The correlation between salinity and AGB clearly indicates that salinity significantly affects the stocks of AGB in the mangrove forest.

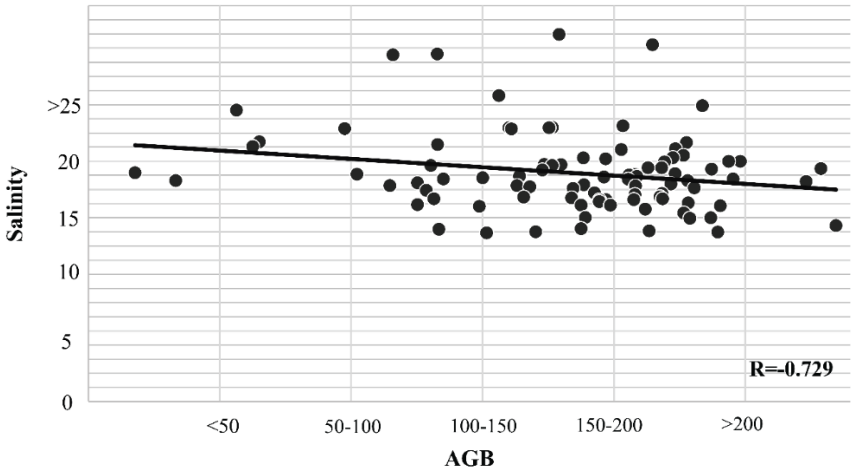

Figure 6. *The correlation between salinity and AGB was examined in Can Gio mangrove forest*

Table 4 and *Figure 6* illustrate the alterations in the extent and AGB of the mangrove forest over time. In the category with AGB less than 50 Mg/ha, the extent has experienced a substantial decline from 6,381.273 ha in 1993 to 537.237 ha in 2023. This may suggest that detrimental factors such as elevated salinity, which adversely affect the growth and survival of vegetation and organisms in that region, have impacted the mangrove forest in this category. In the category with AGB ranging from 50 to 100 Mg/ha, the initial extent was 1,034.282 ha in 1993, decreased to 529.302 ha in 2003, but then rebounded to 3,128.202 ha in 2023. This may indicate a stabilization and recuperation of the mangrove forest in this category following initial changes. For the category with AGB from 100 to 150 Mg/ha, both the extent and AGB have exhibited an ascending pattern over time. The extent has increased from 4,410.474 ha in 1993 to 15,472.083 ha in 2023. This indicates that the mangrove forest in this category possesses a greater tolerance to salinity and a superior ability to recover from initial adverse impacts.

For the categories with AGB from 150 to 200 Mg/ha and >200 Mg/ha, the extent of both categories has significantly decreased in comparison to 1993, with reductions of 44% and 46% respectively (*Table 4*). This is attributed to alterations in the living environment, as escalating salinity over time has considerably modified the living conditions and growth requisites of plant species in the mangrove forest. Generally, the Can Gio mangrove forest flourishes optimally at salinity levels ranging from 5 to 25 ppt, although this is contingent on the particular plant species and their age, which may exhibit varying degrees of salt tolerance. Excessive salinity can diminish biodiversity and exert negative effects on the mangrove forest ecosystem. However, it should be underscored that there exist numerous other factors that can influence AGB in the mangrove forest, and further research is indispensable to acquire a more comprehensive understanding of this correlation.

http://www.aloki.hu ● ISSN 1589 1623 (Print) ● ISSN1785 0037 (Online)
DOI: http://dx.doi.org/10.15666/aeer/2301_16351658

Moreover, in the peripheral regions of mangrove ecosystems, where mangrove species are frequently influenced by elevated salinity levels, the relationship between salinity and AGB becomes increasingly intricate due to anthropogenic activities (*Figure 5*). Human endeavors, including urban expansion, land utilization, and infrastructure development, have exacerbated the incursion of saline water into mangrove habitats, particularly in the face of climate change. This encroachment not only heightens salinity levels but also affects the ecological composition and biodiversity of mangrove forests. The degradation of mangrove regions caused by saline intrusion can significantly reduce their resilience against storms and floods, thus impacting adjacent communities.

Discussion

Mangrove forests play a vital role in the protection and preservation of coastal ecosystems (Jin-Eong, 1995; Herison, 2014). They provide a multitude of ecological services, including coastal protection against waves and storms, water filtration, and the provision of habitat for diverse animal and plant species. Furthermore, they serve as breeding and nursery grounds for various shrimp, fish, and other animal species (Zhang et al., 2012; Thatoi et al., 2013). However, these mangrove forests are currently confronted with several challenges, including climate change, pollution, and resource exploitation (Alongi, 2002; Giri, 2016). One of the crucial factors that impact mangrove forests is the salinity of their environment (Perri et al., 2023). Alterations in salinity levels can lead to changes in vegetation structure, survival rates, and growth patterns within the mangrove forest, thereby affecting AGB (Mitra et al., 2010).

Although the decline in aboveground biomass (AGB) of mangrove forests is influenced by saltwater intrusion, many studies often address these two factors separately (Mitra et al., 2010; Mitra, 2018). Additionally, the lack of consideration for the spatial and temporal relationships between these factors can lead to limitations in comprehending and predicting their intricate interactions (Do et al., 2022b). The intrusion of saltwater can impact soil development and thickness, consequently affecting the growth of vegetation on the ground (Ahmed et al., 2023). Various tree species demonstrate differing degrees of salinity tolerance, leading to a heterogeneous species distribution within mangrove ecosystems. For example, the Avicennia species generally flourish in regions with lower salinity, while Rhizophora species are capable of thriving in more saline conditions (Do et al., 2022b). Variations in salinity, driven by freshwater inflows and climatic variables, can induce shifts in AGB distribution among different species. Additionally, human influences substantially contribute to AGB variations. These influences may lead to a reduction in AGB, particularly in zones significantly impacted by human activity. These interactions may vary over time and space, and disregarding this relationship can compromise the integrity and accuracy of the findings. Some other studies, such as Mitra et al. (2010); and Yoshikai et al. (2022), have examined these changes through field surveys and measurements. However, studies employing conventional methods often yield restricted and non-representative datasets that may be influenced by the survey environment, thereby affecting the reliability of the data (Do et al., 2022b; Pham et al., 2023).

Solar radiation has the potential to alter the spectral characteristics of objects, leading to interference and impacting the quality of signals captured by satellite image sensors (Do, 2024b; Do et al., 2024b). Numerous studies have indicated that post sun-glint correction of satellite images aids in enhancing the quality and precision of analysis and

http://www.aloki.hu ● ISSN 1589 1623 (Print) ● ISSN1785 0037 (Online)
DOI: http://dx.doi.org/10.15666/aeer/2301_16351658

observations, thereby enhancing environmental monitoring and evaluation (Doxani et al., 2013; Chu and Zhang, 2018). However, relying exclusively on Landsat satellite imagery, which offers moderate resolution, may result in the omission of critical details regarding the structure and distribution of plant species, potentially leading to an underrepresentation of AGB, especially in areas with high biomass. To mitigate these challenges, forthcoming research should explore alternative satellite data options, such as Sentinel imagery, which provides a spatial resolution of 10 meters. In the present investigation, the combination of sun glint corrected remote sensing and hybrid models has been utilized to estimate the AGB and salinity of the Can Gio mangrove forest (*Figures 4 and 5*). The outcomes indicate a correlation between AGB and salinity, with AGB showing a tendency to decrease over a 30-year period while salinity tends to increase. Notably, the fringe area and areas with AGB above 150 Mg/ha experienced the most significant decline in AGB. The fringe area represents the direct interface between freshwater and saltwater, where saltwater from the sea floods into the mangrove forest area during high tide, causing a temporary increase in salinity. This cyclic fluctuation in salinity affects the living environment within the mangrove forest.

In this study, XGBoost models and hybrid XGBoost-SVM models were evaluated against each other. The findings reveal that the SVM-XGBoost model consistently outperforms, demonstrating an R^2 accuracy enhancement of nearly 0.2. The SVM, known for its strong classification abilities attributed to well-defined decision boundaries, when paired with XGBoost, improves overall precision by refining features and reducing prediction errors. While XGBoost also shows commendable performance, it frequently does not reach the same level of accuracy as the SVM-XGBoost model, particularly in the context of complex nonlinear relationships. The SVM algorithm-based optimization method has demonstrated its effectiveness when comparing model performance, with both the SVM-XGBoost-1 and SVM-XGBoost-2 models achieving $R^2>0.8$, and a decrease in RMSE from 9.328 and 5.223 to 4.982 and 3.026, respectively (*Table 3*). Similarly, the study conducted by A. N. T. Do et al. (2022b) also revealed that the combination of machine learning models and optimization algorithms led to higher accuracy in predictions. While the hybrid SVM-XGBoost model demonstrates exceptional efficacy, it necessitates meticulous parameter tuning for both models. Improper variable selection may heighten the risk of overfitting.

Moreover, the investigation conducted by Do et al. (2022b) has also unveiled that subsequent to a period of shrimp cultivation in the Can Gio mangrove forest, the ingress and egress points of water suffered erosion, compelling shrimp farmers to relocate to alternative regions, where they proceeded to construct novel embankments and canals in select locations. Consequently, this circumstance resulted in waterlogging and consequent loss of trees. Conversely, within the research site, *Rhizophora apiculata* marina is the dominant tree species in the research area, with an average lifespan of 21 years. However, the planted *Rhizophora apiculata* forest in Can Gio has surpassed the age of 30, with a tree density that exceeds the stipulated regulations. Thus, as salinity levels escalate, the heightened salt concentrations present in the environment adversely impact the structural and functional integrity of the tree cell membranes. Furthermore, aged *Rhizophora apiculata* trees contend for limited supplies of water and nutrients within the mangrove habitat, thereby engendering diminished growth and development, ultimately culminating in a reduction in AGB. Simultaneously, the region characterized by an AGB range of 100 to 150 Mg/ha has demonstrated an upward trajectory over the past three decades, a phenomenon that can be ascribed to the advanced age of the forest

http://www.aloki.hu ● ISSN 1589 1623 (Print) ● ISSN1785 0037 (Online)
DOI: http://dx.doi.org/10.15666/aeer/2301_16351658

and its concomitant decline in health due to factors such as pest infestation, diminished resilience, and competition from mature trees, all of which contribute to a decline in AGB.

Nevertheless, it is important to note that this study exclusively concentrates on the influence of salinity on vegetation within mangrove forests, while mangrove forests themselves constitute intricate ecosystems harboring intricate interactions among diverse plant and animal species. Exploring additional factors, such as the mutual interactions between species and other environmental elements, may yield invaluable insights into the multifaceted interactions and complexity inherent to mangrove forest ecosystems. For instance, increased rainfall generally diminishes soil salinity, thereby enhancing growth conditions for flora such as Avicennia and Rhizophora. In contrast, during arid seasons marked by reduced precipitation, soil and water salinity tend to escalate due to evaporation and a lack of freshwater for diluting salt concentrations. Furthermore, anthropogenic activities, including groundwater extraction, coastal dike construction, and urbanization, can disrupt natural hydrological patterns and elevate soil salinity levels. Similar findings have been reported in research conducted by Do et al. (2022b, 2024b). Enhanced comprehension of how these factors interplay and impact mangrove forests can facilitate the formulation of comprehensive and sustainable strategies for their management. To further develop this research, several directions can be considered. One of them is studying management and conservation strategies for mangrove forests to mitigate the impact of salinity changes. This may encompass investigating the restoration and preservation of mangrove areas that have suffered severe consequences as a result of salinity fluctuations.

The results of this investigation are not only crucial for elucidating the ecological attributes of this ecosystem but also pave the way for potential applications in conservation policy and environmental governance within biosphere reserves. A thorough comprehension of the factors influencing AGB, such as salinity and anthropogenic influences, facilitates the formulation of more scientifically grounded and rational policies. In addition, research focusing on AGB within mangrove ecosystems can play a pivotal role in climate change mitigation strategies. Given that mangroves possess significant carbon storage capabilities, preserving and rehabilitating these areas can contribute to the reduction of greenhouse gas emissions. Initiatives aimed at climate change mitigation can be fortified through the development of mangrove protection programs, thereby yielding enhanced environmental outcomes.

To achieve a more nuanced understanding of mangrove forest dynamics, prospective research could explore the effects of temperature on the growth of tree species inhabiting these ecosystems. Observing seasonal temperature variations and alterations attributable to climate change will offer valuable insights into temperature's influence on biomass and the recovery potential of mangroves. Another critical aspect for investigation is land-use change. Future studies could assess the ramifications of these activities on biomass fluctuations, including the examination of shifts in species composition and their implications for biodiversity.

Conclusion

Over the course of the last three decades, the aboveground biomass (AGB) of mangrove forests has exhibited a downward trajectory, particularly during the time period spanning from 2013 to 2023. It has been established that salinity displays a strong association with this decline, with R=-0.729. These findings underscore the necessity of

http://www.aloki.hu ● ISSN 1589 1623 (Print) ● ISSN1785 0037 (Online)
DOI: http://dx.doi.org/10.15666/aeer/2301_16351658

implementing measures aimed at preserving mangrove forests at the present moment. In the case of dominant species like *Rhizophora apiculata*, which have already reached maturity, prompt reforestation efforts are imperative to ensure their ongoing growth and development. Although the evaluation of the model's performance yielded high results in terms of estimating biomass and salinity in mangrove forests, the current study solely relied on Landsat satellite imagery possessing a moderate spatial resolution. Consequently, the prediction model has not attained absolute accuracy. Subsequent investigations will utilize high-resolution SPOT satellite data to enhance the model's prediction capabilities. Furthermore, the current research has also unveiled that salinity is not the sole factor contributing to the decline in mangrove AGB. Thus, future studies will undertake an assessment to determine and identify the most influential factors impacting the growth of mangrove forests within the study area.

Author contributions. Anh Ngoc Thi Do, Huy Xuan Chu, Toan Quang Le: Formal analysis, Software, Writing-review and editing, Validation. Ngoc Minh Nguyen, Ai Huyen Thi Tong, Huy Quang Bui: Data curation, Writing - Review and Editing. Hai Hoang, Hai Phuc Nguyen, Hieu Duc Nguyen: Investigation, Data curation, Writing-review and editing. All authors have read and agreed to the published version of the manuscript.

Conflicts of Interest. The author declares no conflict of interest.

Data availability. Data will be made available on request.

Acknowledgements. The authors thank anonymous reviewers for their helpful comments and suggestions, which improved this manuscript.

Funding. This research was financially supported by the VAST under the code: QTRU02.08/23-24; Project name: "Adapting sunglint correction algorithm for VNREDSat-1 and Sentinel-2 images using collected insitu dataset from Academier OPARIN 8 cruise".

REFERENCES

[1] Ahmed, S., Sarker, S. K., Friess, D. A., Kamruzzaman, M., Jacobs, M., Sillanpää, M., Naabeh, C. S. S., Pretzsch, H. (2023): Mangrove tree growth is size-dependent across a large-scale salinity gradient. – Forest Ecology and Management 537: 120954.

[2] Alexakis, D. D., Daliakopoulos, I. N., Panagea, I. S., Tsanis, I. K. (2018): Assessing soil salinity using WorldView-2 multispectral images in Timpaki, Crete, Greece. – Geocarto International 33: 321-338. https://doi.org/10.1080/10106049.2016.1250826.

[3] Allbed, A., Kumar, L., Aldakheel, Y. Y. (2014): Assessing soil salinity using soil salinity and vegetation indices derived from IKONOS high-spatial resolution imageries: Applications in a date palm dominated region. – Geoderma 230-231: 1-8. https://doi.org/10.1016/j.geoderma.2014.03.025.

[4] Alongi, D. M. (2002): Present state and future of the world's mangrove forests. – Environmental Conservation 29: 331-349. https://doi.org/10.1017/S0376892902000231.

[5] Biswas, P. L., Biswas, S. R. (2021): Mangrove Forests: Ecology, Management, and Threats. – In: Leal Filho, W., Azul, A. M., Brandli, L., Lange Salvia, A., Wall, T. (eds.) Life on Land, Encyclopedia of the UN Sustainable Development Goals. Springer International Publishing, Cham, pp. 627-640. https://doi.org/10.1007/978-3-319-95981-8_26.

http://www.aloki.hu ● ISSN 1589 1623 (Print) ● ISSN1785 0037 (Online)
DOI: http://dx.doi.org/10.15666/aeer/2301_16351658

[6] Chandra, I. A., Seca, G., Abu Hena, M. K. (2011): Aboveground Biomass Production of *Rhizophora apiculata* Blume in Sarawak Mangrove Forest. – American Journal of Agricultural and Biological Sciences 6: 469-474. https://doi.org/10.3844/ajabssp.2011.469.474.
[7] Chen, T., He, T., Benesty, M., Khotilovich, V., Tang, Y., Cho, H., Chen, K. (2015): Xgboost: extreme gradient boosting. – R package version 0.4-2 1, 1–4.
[8] Chen, T., Guestrin, C. (2016): Xgboost: A scalable tree boosting system. – In: Proceedings of the 22nd Acm Sigkdd International Conference on Knowledge Discovery and Data Mining, pp. 785-794.
[9] Chen, T., He, T., Benesty, M., Khotilovich, V. (2019): Package 'xgboost.'. – R version 90, pp. 1-66.
[10] Chu, M., Zhang, H. (2018): Comparison experiment of sun glint correction method for nearshore high-resolution multispectral satellite images. – In: Ocean Optics and Information Technology. SPIE, pp. 213-222.
[11] Clough, B. F., Scott, K. (1989): Allometric relationships for estimating above-ground biomass in six mangrove species. – Forest Ecology and Management 27: 117-127. https://doi.org/10.1016/0378-1127(89)90034-0.
[12] Davis, E., Wang, C., Dow, K. (2019): Comparing Sentinel-2 MSI and Landsat 8 OLI in soil salinity detection: a case study of agricultural lands in coastal North Carolina. – International Journal of Remote Sensing 40: 6134-6153. https://doi.org/10.1080/01431161.2019.1587205.
[13] Dittmann, S., Mosley, L., Stangoulis, J., Nguyen, V. L., Beaumont, K., Dang, T., Guan, H., Gutierrez-Jurado, K., Lam-Gordillo, O., McGrath, A. (2022): Effects of extreme salinity stress on a temperate mangrove ecosystem. – Frontiers in Forests and Global Change 5: 859283.
[14] Do, T. A. T., Do, A. N. T., Tran, H. D. (2022): Quantifying the spatial pattern of urban expansion trends in the period 1987–2022 and identifying areas at risk of flooding due to the impact of urbanization in Lao Cai city. – Ecological Informatics 101912. https://doi.org/10.1016/j.ecoinf.2022.101912.
[15] Do, A. N. T., Tran, H. D., Ashley, M. (2022a): Employing a novel hybrid of GA-ANFIS model to predict distribution of whiting fish larvae and juveniles from tropical estuaries in the context of climate change. – Ecological Informatics 71: 101780. https://doi.org/10.1016/j.ecoinf.2022.101780.
[16] Do, A. N. T., Tran, H. D., Ashley, M., Nguyen, A. T. (2022b): Monitoring landscape fragmentation and aboveground biomass estimation in Can Gio Mangrove Biosphere Reserve over the past 20 years. – Ecological Informatics 101743. https://doi.org/10.1016/j.ecoinf.2022.101743.
[17] Do, A. N. T., Tran, H. D., Do, T. A. T. (2023): Impacts of urbanization on heat in Ho Chi Minh, southern Vietnam using U-Net model and remote sensing. – Int. J. Environ. Sci. Technol. https://doi.org/10.1007/s13762-023-05118-x.
[18] Do, A. N. T., Tran, H. D. (2023a): Potential application of artificial neural networks for analyzing the occurrences of fish larvae and juveniles in an estuary in northern Vietnam. – Aquat Ecol. https://doi.org/10.1007/s10452-022-09959-5.
[19] Do, A. N. T., Tran, H. D. (2023b): Combining a deep learning model with an optimization algorithm to detect the dispersal of the early stages of spotted butterfish in northern Vietnam under global warming. – Ecological Informatics 102380. https://doi.org/10.1016/j.ecoinf.2023.102380.
[20] Do, A. N. T., Tran, H. D. (2023c): Application of deep learning in assessing the impact of flooding on the endangered freshwater fish Neolissochilus benasi (Cyprinidae) in a northern province of Vietnam. – Aquat Ecol. https://doi.org/10.1007/s10452-023-10056-4.
[21] Do, A. N. T. (2024a): Utilizing a fusion of remote sensing data and machine learning models to forecast flood risks to agriculture in Hanoi City, Vietnam. – Lett Spat Resour Sci 17: 21. https://doi.org/10.1007/s12076-024-00382-y.

http://www.aloki.hu ● ISSN 1589 1623 (Print) ● ISSN1785 0037 (Online)
DOI: http://dx.doi.org/10.15666/aeer/2301_16351658

[22] Do, A. N. T. (2024b): Assessing the Impact of Habitat Fragmentation on the Distribution of Juvenile and Larval Sillago Species in the Ka Long Estuary Located in Northern Vietnam. – Ocean Sci. J. 59: 24. https://doi.org/10.1007/s12601-024-00149-y.
[23] Do, A. N. T., Do, T. A. T., Tran, H. D. (2024a): Distribution of fish larvae and juveniles on salinity in an estuary predicted from remote sensing and fuzzy logic approach. – Aquat Ecol. https://doi.org/10.1007/s10452-024-10119-0.
[24] Do, A. N. T., Do, T. A. T., Van Pham, L., Tran, H. D. (2024b): Assessment of the role of mangroves for Periophthalmus modestus applying machine learning and remote sensing: a case study in a large estuary from Vietnam. – Aquat Ecol. https://doi.org/10.1007/s10452-024-10111-8.
[25] Doxani, G., Papadopoulou, M., Lafazani, P., Tsakiri-Strati, M., Mavridou, E. (2013): Sun glint correction of very high spatial resolution images. – Thales, in Honor of Prof. Emeritus Michael E. Contadakis pp. 329-340.
[26] Fang, L., Liu, Z., Chen, S., Huang, W. (2019): Measuring surface water salinity of Pearl River Estuary by MODIS 250-m imageries. – Journal of Environmental Biology 40: 472-485.
[27] Feller, I. C., Lovelock, C. E., Berger, U., McKee, K. L., Joye, S. B., Ball, M. C. (2010): Biocomplexity in Mangrove Ecosystems. – Annu. Rev. Mar. Sci. 2: 395-417. https://doi.org/10.1146/annurev.marine.010908.163809.
[28] Giri, C. (2016): Observation and monitoring of mangrove forests using remote sensing: Opportunities and challenges. – Remote Sensing 8: 783.
[29] Herison, A. (2014): Coastal conservation strategy using mangrove ecology system approach. – Asian Journal of Scientific Research 7: 513-524.
[30] Huete, A., Justice, C., Liu, H. (1994): Development of vegetation and soil indices for MODIS-EOS. – Remote Sensing of Environment 49: 224-234.
[31] Jennerjahn, T. C., Gilman, E., Krauss, K. W., Lacerda, L. D., Nordhaus, I., Wolanski, E. (2017): Mangrove Ecosystems under Climate Change. – In: Rivera-Monroy, V. H., Lee, S. Y., Kristensen, E., Twilley, R. R. (eds.) Mangrove Ecosystems: A Global Biogeographic Perspective. Springer International Publishing, Cham, pp. 211-244. https://doi.org/10.1007/978-3-319-62206-4_7.
[32] Jin-Eong, O. (1995): The ecology of mangrove conservation & management. – Hydrobiologia 295: 343-351. https://doi.org/10.1007/BF00029141.
[33] Kay, S., Hedley, J. D., Lavender, S. (2009): Sun glint correction of high and low spatial resolution images of aquatic scenes: a review of methods for visible and near-infrared wavelengths. – Remote Sensing 1: 697-730.
[34] Kodikara, K. A. S., Jayatissa, L. P., Huxham, M., Dahdouh-Guebas, F., Koedam, N. (2017): The effects of salinity on growth and survival of mangrove seedlings changes with age. – Acta Botanica Brasilica 32: 37-46.
[35] Laurin, G. V., Balling, J., Corona, P., Mattioli, W., Papale, D., Puletti, N., Rizzo, M., Truckenbrodt, J., Urban, M. (2018): Above-ground biomass prediction by Sentinel-1 multitemporal data in central Italy with integration of ALOS2 and Sentinel-2 data. – JARS 12: 016008. https://doi.org/10.1117/1.JRS.12.016008.
[36] Liang, S., Zhou, R., Dong, S., Shi, S. (2008): Adaptation to salinity in mangroves: Implication on the evolution of salt-tolerance. – Sci. Bull. 53: 1708-1715. https://doi.org/10.1007/s11434-008-0221-9.
[37] Lyzenga, D. R., Malinas, N. P., Tanis, F. J. (2006): Multispectral bathymetry using a simple physically based algorithm. – IEEE Transactions on Geoscience and Remote Sensing 44: 2251-2259.
[38] Mitra, A., Chowdhury, R., Sengupta, K., Banerjee, K. (2010): Impact of salinity on mangroves. – Jour. Coast. Env 1.
[39] Mitra, A. (2018): Salinity: A primary growth driver of mangrove forest. – Sustainable Forestry 1.

http://www.aloki.hu ● ISSN 1589 1623 (Print) ● ISSN1785 0037 (Online)
DOI: http://dx.doi.org/10.15666/aeer/2301_16351658

[40] Nam, V. (2019): Biomass estimation and mapping of can GIO mangrove biosphere reserve in south of viet nam using ALOS-2 PALSAR-2 data. – Applied Ecology and Environmental Research 17: 15-31.
[41] Noor, T., Batool, N., Mazhar, R., Ilyas, N. (2015): Effects of siltation, temperature and salinity on mangrove plants. – European Academic Research 2: 14172-14179.
[42] Parida, A. K., Das, A. B., Sanada, Y., Mohanty, P. (2004): Effects of salinity on biochemical components of the mangrove, *Aegiceras corniculatum*. – Aquatic botany 80: 77-87.
[43] Perri, S., Detto, M., Porporato, A., Molini, A. (2023): Salinity-induced limits to mangrove canopy height. – Global Ecol Biogeogr 32: 1561-1574. https://doi.org/10.1111/geb.13720.
[44] Pham, T. D., Yoshino, K. (2017): Aboveground biomass estimation of mangrove species using ALOS-2 PALSAR imagery in Hai Phong City, Vietnam. – Journal of Applied Remote Sensing 11: 026010-026010.
[45] Pham, V. T., Do, T. A. T., Tran, H. D., Do, A. N. T. (2023): Classifying forest cover and mapping forest fire susceptibility in Dak Nong province, Vietnam utilizing remote sensing and machine learning. – Ecological Informatics 79:102392.
[46] Pham, T. V., Do, T. A. T., Tran, H. D., Do, A. N. T. (2023): Assessing the impact of ecological security and forest fire susceptibility on carbon stocks in Bo Trach district, Quang Binh province, Vietnam. – Ecological Informatics 74: 101962. https://doi.org/10.1016/j.ecoinf.2022.101962.
[47] Pham, T. V., Thi Do, T. A., Tran, H. D., Thi Do, A. N. (2024): Assessing groundwater potential for mitigating salinity issues in agricultural areas of southern Dong Nai province, Vietnam. – Groundwater for Sustainable Development 25: 101177. https://doi.org/10.1016/j.gsd.2024.101177. https://doi.org/10.1016/j.ecoinf.2023.102392.
[48] Sharifi, A., Hosseingholizadeh, M. (2020): Application of Sentinel-1 Data to Estimate Height and Biomass of Rice Crop in Astaneh-ye Ashrafiyeh, Iran. – J Indian Soc Remote Sens 48: 11-19. https://doi.org/10.1007/s12524-019-01057-8.
[49] Shiau, Y.-J., Lee, S.-C., Chen, T.-H., Tian, G., Chiu, C.-Y. (2017): Water salinity effects on growth and nitrogen assimilation rate of mangrove (Kandelia candel) seedlings. – Aquatic Botany 137: 50-55.
[50] Suárez, N., Medina, E. (2005): Salinity effect on plant growth and leaf demography of the mangrove, *Avicennia germinans* L. – Trees 19: 722-728. https://doi.org/10.1007/s00468-005-0001-y.
[51] Thatoi, H., Behera, B. C., Mishra, R. R. (2013): Ecological role and biotechnological potential of mangrove fungi: a review. – Mycology 4: 54-71.
[52] Tran, P. H., Nguyen, A. K., Liou, Y.-A., Hoang, P. P., Nguyen, H. T. (2018): Estimation of Salinity Intrusion by Using Landsat 8 OLI Data in The Mekong Delta, Vietnam. – https://doi.org/10.20944/preprints201808.0301.v1.
[53] Van Pham, T., Do, A. N. T., Do, T. A. T. (2024): Evaluation of Aboveground Biomass in Mangrove Biosphere Reserves from 1993 to 2023 Under the Influence of Landscape Fragmentation. – J Indian Soc Remote Sens. https://doi.org/10.1007/s12524-024-02027-5.
[54] Vermeulen, D., van Niekerk, A. (2016): Evaluation of a WorldView-2 image for soil salinity monitoring in a moderately affected irrigated area. – J. Appl. Remote Sens 10: 026025. https://doi.org/10.1117/1.JRS.10.026025.
[55] Ward, R. D., Friess, D. A., Day, R. H., Mackenzie, R. A. (2016): Impacts of climate change on mangrove ecosystems: a region by region overview. – Ecosyst Health Sustain 2: e01211. https://doi.org/10.1002/ehs2.1211.
[56] Westin, L., Nissling, A. (1991): Effects of salinity on spermatozoa motility, percentage of fertilized eggs and egg development of Baltic cod (Gadus morhua), and implications for cod stock fluctuations in the Baltic. – Mar. Biol. 108: 5-9. https://doi.org/10.1007/BF01313465.

http://www.aloki.hu ● ISSN 1589 1623 (Print) ● ISSN1785 0037 (Online)
DOI: http://dx.doi.org/10.15666/aeer/2301_16351658

[57] Yoshikai, M., Nakamura, T., Suwa, R., Sharma, S., Rollon, R., Yasuoka, J., Egawa, R., Nadaoka, K. (2022): Predicting mangrove forest dynamics across a soil salinity gradient using an individual-based vegetation model linked with plant hydraulics. – Biogeosciences 19: 1813-1832.
[58] Zhang, K., Liu, H., Li, Y., Xu, H., Shen, J., Rhome, J., Smith III, T. J. (2012): The role of mangroves in attenuating storm surges. – Estuarine, Coastal and Shelf Science 102: 11-23.

http://www.aloki.hu ● ISSN 1589 1623 (Print) ● ISSN1785 0037 (Online)
DOI: http://dx.doi.org/10.15666/aeer/2301_16351658